International Journal of Biological, Life and Agricultural Sciences
ISSN: 2415-6612
Vol:11, No:1, 2017

Passive Neutralization of Acid Mine Drainage Using Locally Produced Limestone

Reneiloe Seodigeng, Malwandla Hanabe, Haleden Chiririwa, Hilary Rutto, Tumisang Seodigeng

Abstract**—**Neutralisation of acid-mine drainage (AMD) using limestone is cost effective, and good results can be obtained. However, this process has its limitations; it cannot be used for highly acidic water which consists of Fe(III). When Fe(III) reacts with $CaCO_3$, it results in armoring. Armoring slows the reaction, and additional alkalinity can no longer be generated. Limestone is easily accessible, so this problem can be easily dealt with. Experiments were carried out to evaluate the effect of PVC pipe length on ferric and ferrous ions. It was found that the shorter the pipe length the more these dissolved metals precipitate. The effect of the pipe length on the hydrogen ions was also studied, and it was found that these two have an inverse relationship. Experimental data were further compared with the model prediction data to see if they behave in a similar fashion. The model was able to predict the behaviour of 1.5m and 2 m pipes in ferric and ferrous ion precipitation.

Keywords**—**Acid mine drainage, neutralization, limestone, modeling.

I. Introduction

THE mining industry has played a very big role in the stabilization of the South African (SA). SA started exporting coal in the early 1970's. The major consequence associated with the mining of coal is that of AMD (an unintended consequence facing the mining industry world-wide). Even though other mineral mining can cause AMD, coal mining remains the number one culprit. As the demand of coal increases, so is the problem of AMD, making it to be a growing environmental crisis [1], and coal mining remains the main culprit in the production of AMD [2]. AMD is mainly caused when iron sulphide is exposed to oxidation conditions. Abundant and cheap coal reserves will therefore almost certainly remain SA's most important energy resource for at least the next 75 years [3].

Active and passive neutralisations of AMD using limestone are some of the treatment methods available for use. Active neutralisation is characterised by agitation, requires constant maintenance, and is relatively expensive, whereas passive neutralisation is simple, no agitation is required, no/less maintenance is required, and cheap to use [4]. For the purpose of this study, passive neutralisation of AMD will be conducted using limestone. Limestone has a neutralisation efficiency of 30%, so it requires large doses to be more efficient. The overall reaction of metal-acid wastewater neutralization process by limestone is given by (1):

$$CaCO_3 + H_2SO_4 \rightarrow CaSO_4 + CO_2 + H_2O \quad (1)$$

Limestone is widely used, economically friendly, easily accessible, has low maintenance costs, and requires minimum monitoring. Yet this process has limitations, it cannot be used for highly acidic water which consists of Fe (III) ions. When Fe (III) ions react with $CaCO_3$, it produces impermeable metal hydroxide coating widely known as armoring [1]. The disadvantages of this reagent include slow rate of dissolution, and its effectiveness decreases with time. Previous studies of armor formation have been conducted by several researchers who investigated the effect of armoring limestones on acid mine neutralisation with limestones, and concluded that even after armoring, limestone was still partly effective in acid neutralization [5]. Few studies address the composition of armor coating on limestones in AMD neutralisation application, armor coating composed of metal oxyhydroxides and Ca sulfate (Gypsum). Rutto et al. described the gypSLIM process that can be used for processing gypsum into sulphur and $CaCO_3$ [6].

The three main objectives of this work were to investigate the effect of pipe length on ferric and ferrous ion precipitation, to model the diffusion of H^+ ions, and to model the diffusion and precipitation of ferric and ferrous ions.

II. Experimental

A. Materials

Limestone was obtained from Phalaborwa Mining Company (PMC). Raw AMD was obtained from the East Rand of Johannesburg. Barium diphenylamine sulphonate, potassium dichromate, 32% hydrochloric acid, 98% sulphuric acid, and starch indicator were bought from Merck South Africa.

Reneiloe Seodigeng, Hilary Rutto and Tumisang Seodigeng are with the Department of Chemical Engineering, Vaal University of Technology, RSA (e-mail: renematlou@gmail.com, hilaryr@vut.ac.za, tumisangs@vut.ac.za).

Malwandla Hanabe was with the Department of Chemical Engineering, Vaal University of Technology, RSA (e-mail: mahanabe@gmail.com).

Haleden Chiririwa is with the Centre for Renewable Energy and Water, Vaal University of Technology, RSA (e-mail: harrychiririwa@yahoo.com).

B. Equipment Set-Up

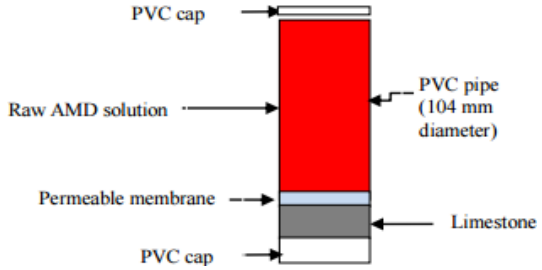

Fig. 1 In-situ AMD neutralization laboratory setup

C. Experimental Procedure

A PVC pipe of length 2 m and 104-mm inside diameter was used to conduct the experiment. 17L of raw AMD was loaded into the column; 220 g of limestone was put inside a stocking and dropped into the column. The amount of limestone was calculated according to the sulphur content in the AMD solution. Samples were drawn from different column lengths (1 m, 1.5 m, and 2 m) at time interval of 24 hours. The concentration of ferrous and ferric ions was obtained by using titration method, and the pH was determined by using a pH meter.

D. Analytical Methods

Titration was used for the purpose of this study to determine the concentration of ferrous and ferric irons.

1. Ferrous Ion Titration

Barium diphenylamine sulphonate indicator: 1 g of barium diphenylamine sulphate was dissolved in distilled water and made to volume of 200 ml. 0.1M Potassium dichromate solution ($K_2Cr_2O_7$): The mass of 0.49033 g of $K_2Cr_2O_7$ was accurately weighed and then transferred to 100 ml volumetric flask. The volume was topped up with distilled water. 20 ml of AMD sample from 0.5 m, 1 m, and 1.5 m pipes was poured into 250 ml beakers, and 20 ml of mist acid was added in the solution for further dissolving the metals in the solution. Two to three drops of barium diphenylamine sulphonate indicator solution were added in the solution. The concentration of 0.1 M of potassium dichromate solution was poured in the 50-ml burette prior titration of the AMD sample. Ferrous ion was detected when the solution turned to intense purple or violet blue colour.

2. Ferric Iron Determination

A sample of 20 ml AMD solution was transferred into a 250-ml beaker and it was diluted with distilled water to approximately 50 ml. 12 ml of concentrated hydrochloric acid and 2 to 3 g of potassium iodide crystals were added to the solution. After the reagents had been added, the sample was placed in the dark room or cardboard for 5 minutes. The blank solution was prepared in the same manner as the AMD, but for the blank, there was no AMD sample added in the solution. The standard solution was prepared using 10 ml of 0.375 N potassium iodide solutions, 50 ml of distilled water, and 10 ml of 25% sulphuric acid and 10 ml of 10% potassium iodide solution in the 250ml beaker. After 5 minutes, the AMD and the blank sample were taken out of the cardboard for titration. Prior to titration 20ml of starch solution indicator was poured in the AMD, blank sample, and standard solution and the solution change to dark blue colour. The concentration of 0.15 N sodium thiosulphate solutions was poured in the 50-ml burette prior titration of AMD sample, blank and standard solution. Titration volume was recorded when the colour changed from dark blue to colourless.

E. Modelling Approach

The pH was used to determine the hydrogen ion concentration at a given time. Fick's law was applied to a differential length segment to model the diffusion of hydrogen ions through points A, B, and C as shown in Fig. 2. The concentration of hydrogen ions can be determined by (2):

$$[H^+] = [H_B^+] + D_H \frac{\Delta T}{\Delta x^2}([H_A^+] - [H_B^+]) - ([H_B^+] - [H_C^+]) \quad (2)$$

where: $[H^+]$: Concentration of the hydrogen ions at a given time; $[H_B^+]$: Concentration of hydrogen ions within the differential change in length of the tube; $[H_A^+]$: Concentration of hydrogen ions entering the differential change of length of tube; $[H_C^+]$: Concentration of hydrogen ions leaving the differential length of tube; D_H: Diffusion coefficient of hydrogen ions; ΔT: Change in time for the diffusion of ions; Δx^2: Differential change in length squared.

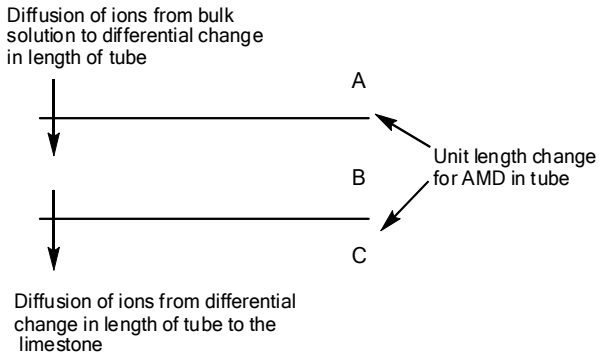

Fig. 2 Representation of diffusion through two imaginary planes

F. Experimental Design

TABLE I
EXPERIMENTAL DESIGN

Constants	Independent Variable	Dependent variable
Limestone (220 g)	Pipe length (1 m,1.5 m, and 2m)	pH
Sample volume (20 ml)	Time (1 day)	$[H^+]$
		$[Fe^{2+}]$
		$[Fe^{3+}]$

Experimental design constants, independent, and dependent variables are shown in Table I.

III. RESULTS AND DISCUSSION

XRD results showed that limestone is calcite-rich with less than 3% mineral impurities. Samples were drawn from three pipe lengths; namely, 1 m, 1.5 m, and 2 m. Analyses were carried out on the samples to determine the rate of AMD

neutralisation, the rate of hydrogen ion diffusion and the rate of the ferric and ferrous ion diffusion and precipitation. The results presented are of a period of 24 days.

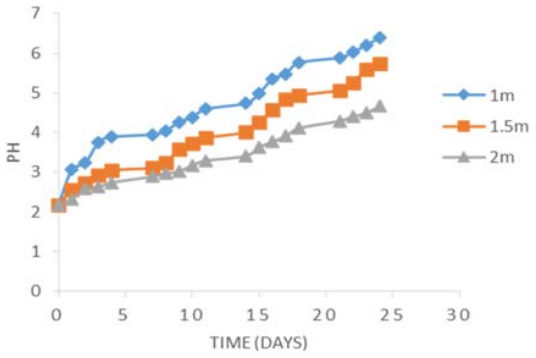

Fig. 3 The change of [H^+] (pH) with time

The data represented by Fig. 3 show direct proportionality between pH and time for all the column lengths. The pH gradient agrees with expectations, as neutralisation starts at the surface of the limestaone and proceeds to the top of the column. Fig. 4 indicates that the neutralisation process is much faster when the length is lower in this case at column length of 1 m, this is due to the fact that it takes less time for the AMD to react with the dissolving limestone surface. These results also imply that it takes longer to neutralise the AMD at the top of the column than it takes to neutralise the middle of the column. The results also show that, in a period of 24 days, the 1 m, 1.5 m, and 2-m column lengths were at the pH of 6.39, 5.74, and 4.67, respectively. The initial pH was 2.18. pH is related to the hydrogen ions, as the hydrogen ions decrease the pH rises. Fig. 4. shows the rate of hydrogen diffusion.

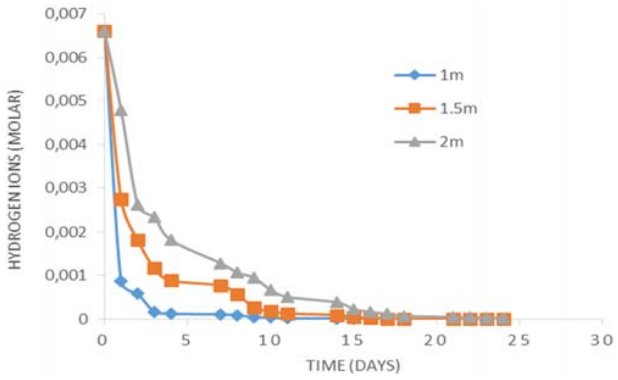

Fig. 4 Rate of H^+ diffusion

The experimental data shown in Fig. 4 indicate how the acidity rate of the AMD decreases for all the column lengths. This is due to the alkalinity provided by the limestone at a pH >12. Mass diffusion occurs between the hydrogen ions and calcite ions due to concentration gradient (hydrogen ions at high concentration moves towards calcite at low concentration). Fig. 4 also shows that as the time progresses the amount of hydrogen ions reaches zero, when the concentration of the hydrogen ions is at zero, the AMD cannot be neutralised further (AMD has reached zero buffering capacity), this also supports the argument that AMD at 1 m neutralise faster than the other lengths. As can be seen, it reaches zero before the other lengths.

AMD contains dissolved metals. In this project, we are focused on precipitating iron since it is dominant, and AMD is mainly formed by the oxidation and hydrolysis of pyrite (Fe_2S). Figs. 5 and 6 illustrate the rate at which iron (II) and iron (III) precipitate, respectively.

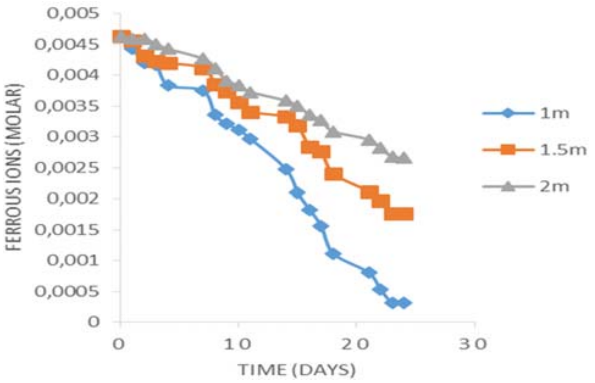

Fig. 5 Rate of precipitation of Fe^{2+}

Fig. 5 shows how ferrous ions precipitate with time for all three different sampling points. It was observed that the 1-m length precipitates faster than 1.5 m and 2-m length, this is because the rate of iron precipitation is pH dependent (as the pH increases so does the rate of iron precipitation). Iron starts to precipitate at a pH of 3.5-6, this further supports the observation regarding the 1-m pipe length, as it reaches 3.5 first between day 2 and 3. Fig. 5 further shows that ferrous ions do not completely precipitate since the buffering capacity of the hydrogen ions has reached zero.

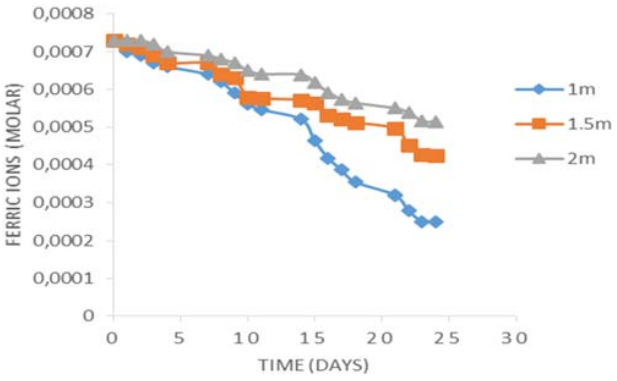

Fig. 6 Rate of precipitation of Fe^{3+} ions

Fig. 6 indicates how ferric ions precipitate with time for the three pipe lengths. It is observed that ferric ions at a length of 2 m are almost linear and stagnant, implying that less ferric ions precipitate. As the length of the column decreases, we experience more ferric ions precipitating, even though it does not completely precipitate, but it shows progress. Ferric ions are

problematic in the neutralisation of AMD using limestone as they tend to passivate the limestone, slowing dissolution rate.

A. Modelling Results

The model was run for similar days as the experiment, to predict the rate at which hydrogen ions will diffuse and the rate at which ferrous and ferric ions will precipitate. Figs. 7-13 clearly illustrate the findings.

1. Modelling of H^+ Ions

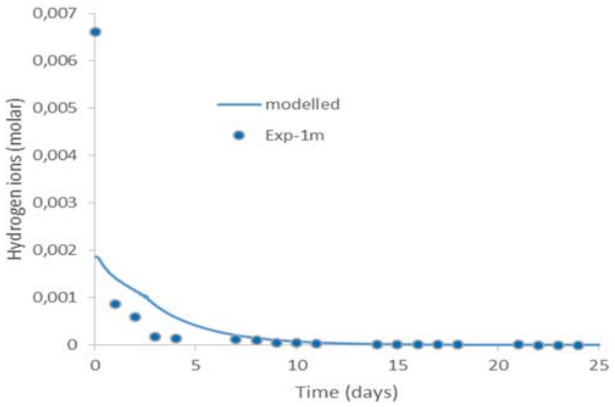

Fig. 7 Experimental data and model results of H^+ against time for 1-m length

Fig. 7 shows the diffusion of hydrogen ions for 1m sampling length. The experimental data and modelling curve show an inverse relationship between hydrogen ions concentration and time. The experimental data for the first four days do not lie on the model curve. In both results (model and experimental), the diffusion of hydrogen ions decreases with time, but the experimental data at the first four days do not lie in the model curve, then as the days proceed, they lie perfectly in the model curve. The model used can be utilised for the diffusion of hydrogen ions in AMD with the length of 1 m. The sum of the square error for Fig. 6 is 0.13.

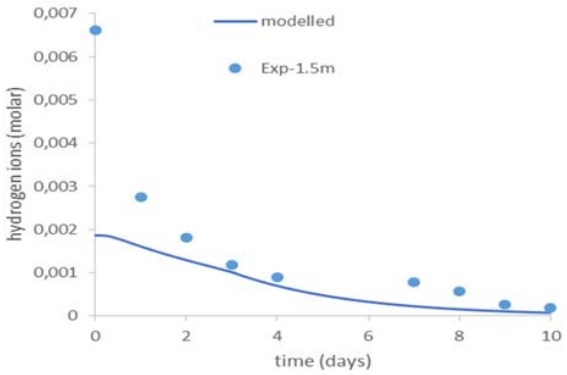

Fig. 8 Experimental data and model results of H^+ against time for 1.5-m length

Fig. 8 shows the diffusion of hydrogen ions for 1.5-m sampling length. In both results, the diffusion of hydrogen ions decreases with time, but the experimental data do not lie in the model curve. The experimental data and the modelled data behave in similar fashion, they do not vary much. The reason why the experimental does not lie on the curve can be because of different diffusion coefficient; the modelled curve can be taken a little bit up by decreasing the diffusion coefficient of the model. The model used can be utilised for the diffusion of hydrogen ions in AMD with the length of 1.5 m with SSE of 0.34.

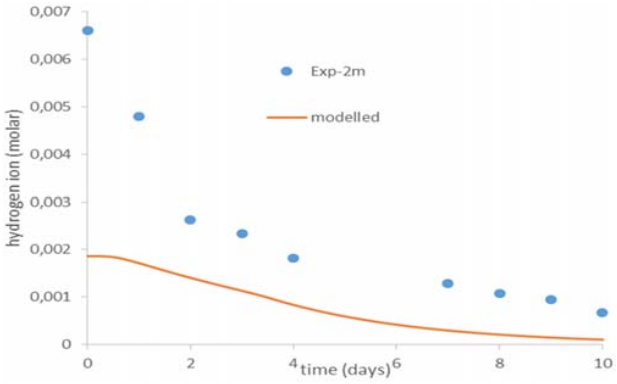

Fig. 9 Experimental data and model results of H^+ against time for 1.5-m length

Fig. 9 shows the diffusion of hydrogen ions for 1-m sampling length. In both results, the diffusion of hydrogen ions decreases with time, but the experimental data do not lie on the model curve even though they both behave in an exponential fashion. The same argument holds as that of Fig. 10 with regard to adjusting the modelling curve. The model can be utilised for the diffusion of hydrogen ions in AMD with the length of 1 m. The sum of the square error for Fig. 9 is 0.76.

2. Modelling of Ferrous Ions

Fig. 10 shows the precipitation of ferrous ions for 1-m sampling length. In both results the precipitation of ferrous ions decreases with time; for the first 10 days, the experimental data behave in a similar fashion with the modelled data, which is exponential, and from day 15 the experimental data show a linear behaviour.

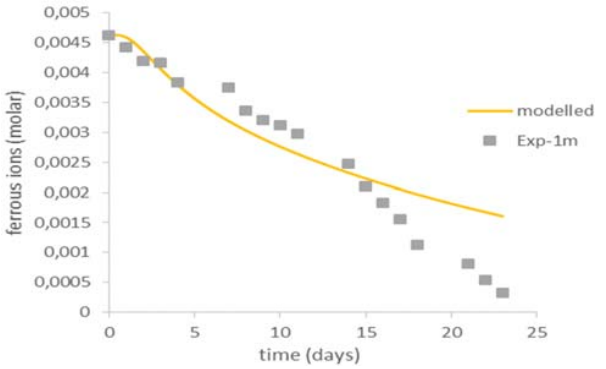

Fig. 10 Experimental data and model results of Fe^{2+} against time for 1-m length

The difference in behaviour may be due to reaction disturbance by moving the column during cleaning in the laboratory which results in active treatment. SSE value for Fig. 10 is 0.84 which is relatively high but less than 1; this model can still be utilised for neutralising AMD with the length of 1 m.

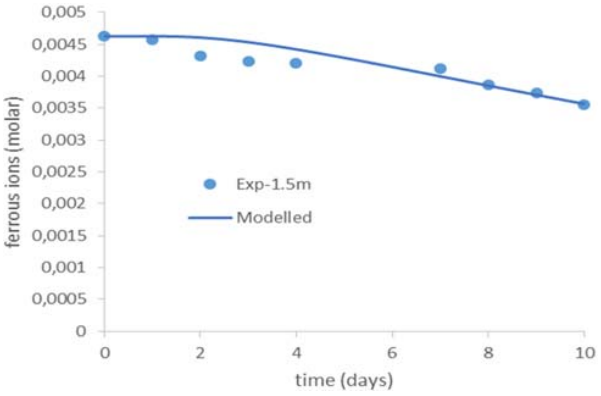

Fig. 11 Experimental and modelling data of [Fe^{2+}] against time for 1.5-m length

Fig. 11 shows the precipitation of ferrous ions for 1.5-m sampling length. In both results, the precipitation of ferric ions decreases with time, four of the experimental data do not lie on the curve, but they are still close enough to the modelled curve resulting in SSE value of 0.023 which is greater than zero and less than 1. The model used can be utilised for the precipitation of ferrous ions in AMD with the length of 1.5 m due to small SSE value and similar behaviour of the modelled data and experimental data.

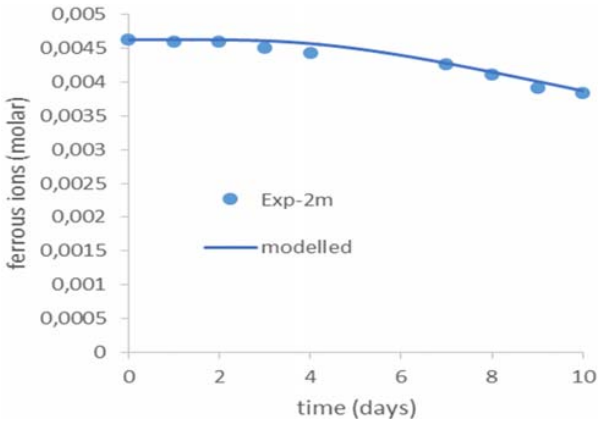

Fig. 12 Experimental and modelling data of [Fe^{2+}] against time for 2-m length

Fig. 12 shows the precipitation of ferrous ions for 2-m sampling length. In both results, the precipitation of ferric ions decreases with time. The experimental data lie perfectly on the model curve resulting in SSE value of 0.01 which is closer to zero, with one point slightly below the model curve. The model used can be utilised for the precipitation of ferrous ions in AMD with the length of 2 m.

3. Modelling of Ferric Ions

Fig. 13 shows the precipitation of ferric ions for 1-m sampling length. In both results, the precipitation of ferric ions decreases with time, but the experimental data are far from the modelled data resulting in huge SSE value of 2.64 which is way greater than zero. The model used cannot be properly utilised for neutralising AMD with a PVC pipe of 1 m long. The modelled data further show noise at day 11, and this is attributed to the fact that Microsoft excel VBA does not handle residues well.

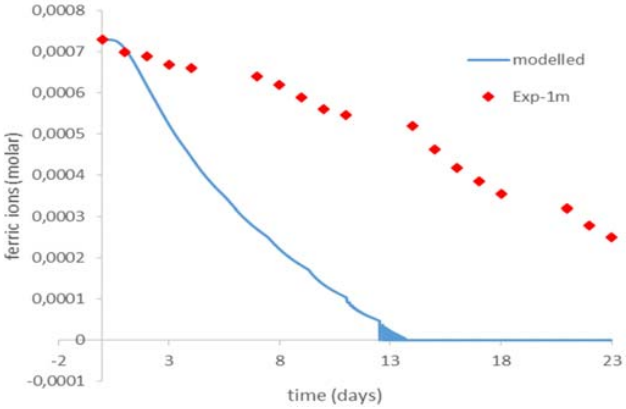

Fig. 13 Experimental and modelling data of [Fe^{3+}] against time for 1-m length

IV. Conclusion

AMD can be passively neutralised using locally produced limestone from Phalaborwa Mining Company (PMC). Ferric and ferrous ions require high pH level for them to completely precipitate. The diffusion/precipitation model is very efficient and it was able to predict the behaviour of ferrous ions for the 1.5-m and 2-m PVC pipes because of their small value of the sum of square error. The model however requires further modifications, to cater for residuals. The results further showed that 1 m was the most optimal length for the neutralisation and precipitation of ferric and ferrous ions, implying an inverse relationship between the pipe length and neutralisation capacity.

Acknowledgments

The authors would like to acknowledge the Department of Chemical Engineering at Vaal University of Technology for funding this project.

References

[1] Hammarstrom, J. M., Sibrell, L. P., and Belkin, H. V., 2003. Characterisation of limestone reacted with acid-mine drainage in a pulsed limestone bed treatment system at the Friendship Hill National Historical Site, Pennsylvania, USA.
[2] Louis, R.B., Aubertin, M., Poirier, C., and Bussiere, B., 2002. On the use of limestone drains in the passive treatment of acid-mine drainage. Montreal, Canada.
[3] Engelbrecht, A.D., 2007. Investigation into the gasification characteristics of South African power station coals, CSIR, Pretoria, South Africa.

[4] Schmid, K. L., Sharpe, W. E., 2002. Passive treatment methods for acid water Pennsylvania. PennState college of Agricultural Science Agricultural Research and Cooperative Extension.
[5] Ziemkiewics, P., Skousen, J., and Lovett, R., 1997. Acid-mine drainage treatment with armored limestones in open limestones channels. J. Environ. Qual. 26: 1017-1024.
[6] Rutto, S., Maree, J.P., Zvinowanda, C.W., Louw, W.J., and Koslesnikov, A.V., 2011. Thermal studies on gypsum in a pilot-scale, rotary kiln. Proc. Water in the South African institute of mining and metallurgy, 01-06 March 2015.